

MsCGAN: Multi-scale Conditional Generative Adversarial Networks for Person Image Generation

Wei Tang^{*}, Teng Li [†], Fudong Nian[‡], Meng Wang[§]

^{*} [†] Anhui University, HeFei, China

[‡] Hefei University, HeFei, China

[§] Hefei University of Technology, HeFei, China

Abstract—To synthesize high quality person images with arbitrary poses is challenging. In this paper, we propose a novel Multi-scale Conditional Generative Adversarial Networks (MsCGAN), aiming to convert the input conditional person image to a synthetic image of any given target pose, whose appearance and the texture are consistent with the input image. MsCGAN is a multi-scale adversarial network consisting of two generators and two discriminators. One generator transforms the conditional person image into a coarse image of the target pose globally, and the other is to enhance the detailed quality of the synthetic person image through a local reinforcement network. The outputs of the two generators are then merged into a synthetic, discriminant and high-resolution image. On the other hand, the synthetic image is down-sampled to multiple resolutions as the input to multi-scale discriminator networks. The proposed multi-scale generators and discriminators handling different levels of visual features can benefit to synthesizing high resolution person images with realistic appearance and texture. Experiments are conducted on the Market-1501 and DeepFashion datasets to evaluate the proposed model, and both qualitative and quantitative results demonstrate superior performance of the proposed MsCGAN.

Index Terms—Person Image Generation, Multi-scale Discriminators, Generative Adversarial Networks, Image Synthesis.



1 INTRODUCTION

To generate high-resolution and photo-realistic person image with arbitrary poses is important in multimedia and computer vision for its wide range of applications such as data augmentation in person re-identification (re-ID) [1], person image editing or inpainting [2] and video forecasting [3]. Various methods have been proposed to handle this problem, such as variational autoencoders (VAE) [4], autoregressive models (ARMs) [5], and generative adversarial networks (GANs) [6]. Recent works mostly focus on GANs due to its impressive results [2] [7] [8] [9] [10].

From the perspective of the prior knowledge they used, existing GANs based person image generation methods can be categorized into two groups. The first is global pose-guided [7], [8], [9] and the second is segmentation-guided multi-stage strategy [10]. The former is to synthesize the target person image through a global model by inputting the conditional person image and the human pose estimation simultaneously. The later is to parse the conditional person image into foreground, background and pose information, then synthesize the target image using multi-stage models. Although pose-guided person image generation methods can be accurate regarding target human poses, they usually neglect the detailed appearance and the texture information of the conditional person images. On the other hand, segmentation-guided multi-stage person image generation techniques can preserve appearance and texture features of the conditional person image more completely. However,



Fig. 1. Synthetic samples by the proposed MsCGAN on public datasets. The inputs of MsCGAN are a conditional person image and a novel pose, the output of it is a synthetic person image with the target pose, which appearance and the texture information are also consistent with the conditional person image. Single-scale-1 and Single-scale-2 are variants of the presented MsCGAN (Please refer to the main text).

most multi-stage models are complex and difficult to train. Moreover, the pose accuracy of resulted image by these models is still far from expectation. In many cases above mentioned methods are still problematic to produce person image with precise pose and preserve appearance details simultaneously.

In this paper, we propose a novel Multi-scale Conditional Generative Adversarial Networks (MsCGAN) for person image generation. As illustrated in Fig. 1, the inputs

are conditional person image and target pose. Our goal is to synthesize person image with the target pose, whose appearance and the texture information are also consistent with the conditional person images. MsCGAN is based on pose guidance so that it can synthesize person images with a high pose accuracy. Meanwhile, MsCGAN contains two strategies to ensure the visual quality of generated images to be consistent with the conditional person image. One is the using of global-to-local generators, which generate a coarse image of the specific pose globally, and then refine the coarse image locally. The other is that we adopted multi-scale discriminators, which are expected to discriminate the generated image and its down-sampled images respectively, to handle the visual features on multiple levels.

To simultaneously handle global structure and local appearance of the person image, the proposed generation process is divided into two stages corresponding to the two sub-generators. At stage-I, global structure generator adopts a segmentation model similar to U-Net [11] that combines the residual blocks and generates a coarse image with the pose of the target person image. At stage-II, local reinforcement generator network outputs an appearance difference map between conditional person image and the result of stage-I. Furthermore, to compensate for the background change between conditional person image and target person image, we introduce a background loss both at stage-I and stage-II. The outputs of the two generators are merged into a synthetic image. Furthermore, to consider visual appearance of generated images on multi-resolution, we adopt multi-scale discriminators that discriminate different resolution synthetic images. The weighted sum of results of the proposed two discriminators is considered as the final discriminant result.

Compared with existing methods, our proposed model has several advantages: 1) Joint global generation and local refinement can model both the accuracy and quality of the synthetic image simultaneously. 2) Different resolution images contain different level visual features, so the proposed multi-scale discriminators can increase the receptive field of the discriminator. 3) The combination of the global-to-local generators and multi-scale discriminators ensure that the synthetic person images have the target pose and more detailed appearance features than existing methods. Some examples are shown in Fig. 1. The proposed model is evaluated on the benchmark person re-identification dataset Market-1501 [12] with image resolution of 128×64 , as well as the fashion dataset DeepFashion [13] with image resolution of 256×256 . Moreover, we compare our results to the results of the state-of-the-art methods to demonstrate the effectiveness.

The main contributions of our work are summarized as follows:

- We propose a novel MsCGAN model for person pose image generation, which is able to handle more detailed appearance and texture information while synthesizing high-quality and realistic person images with arbitrary poses.
- The proposed global-to-local generating strategy, as well as multi-scale discriminators, can be widely used in GANs based image or video synthesis.

- The proposed MsCGAN is an end-to-end model, which is more compact than segmentation-guided multi-stage methods, and it achieves much superior performance than existing methods on the benchmark Market-1501 and DeepFashion datasets.

The rest of the paper is organized as follows. In Section 2, the related work is reviewed. Section 3 introduces the details of the proposed MsCGAN. In Section 4, we report and analyze extensive experimental results. Finally, we conclude the paper with future work in Section 5.

2 RELATED WORK

In this section, we briefly review the existing literature which closely related to the presented MsCGAN.

Person image generation is an area of great interests in the fields of vision and multimedia. Recent researches are mostly based on GANs, and many of them have achieved impressive results [7] [8] [9] [2] [10]. From perspective of the prior knowledge they used, existing GANs based person image generation framework can be categorized into two groups.

The first is generation based on global pose guidance [9] [7] [2] [8] which synthesizes the target image by inputting the conditional person image and the human pose estimation. Pumarola et al. [9] propose an unsupervised method for human body image generation with arbitrary poses. This method reconstructs the input image to alleviate the problems caused by the unpaired data. Unlike [9], pose guided person generation network (PG^2) [7] applies paired data to perform training based on pose guided person image generation. PG^2 generate person images in a divide-and-conquer way. Si et al. [2] propose a pose-based human image synthesis method which can keep the pose unchanged in novel viewpoints by separating foreground and background of the input person image. To synthesize more plausible human poses, Siarohin et.al [8] apply deformable skip connections and compute a set of affine transformations to approximate joint deformations.

The second is multi-stage generations based on segmentation [10] which decomposes the conditional person image into foreground, background and pose, and synthesize the target image by using multi-stage models. Si et al. [2] also separate foreground and background of the input person image to synthesize person image with novel viewpoints unchanged pose.

From the above mentioned two categories of methods, we can draw the following conclusions. The method of generation based on pose guidance is good regarding accuracy of generated pose. The multi-stage generations method based on segmentation can preserve the visual appearance features and texture information better. However, the first category misses detailed features of the appearance and the texture information of the conditional person images, while the second is poor in pose accuracy of generated image. Moreover, the multi-stage models are complex and difficult to train.

In this paper, we propose a novel method modelling human pose to synthesize image with global-to-local generators and multi-scale discriminators model. Since our proposed method is based on pose guidance, and we use

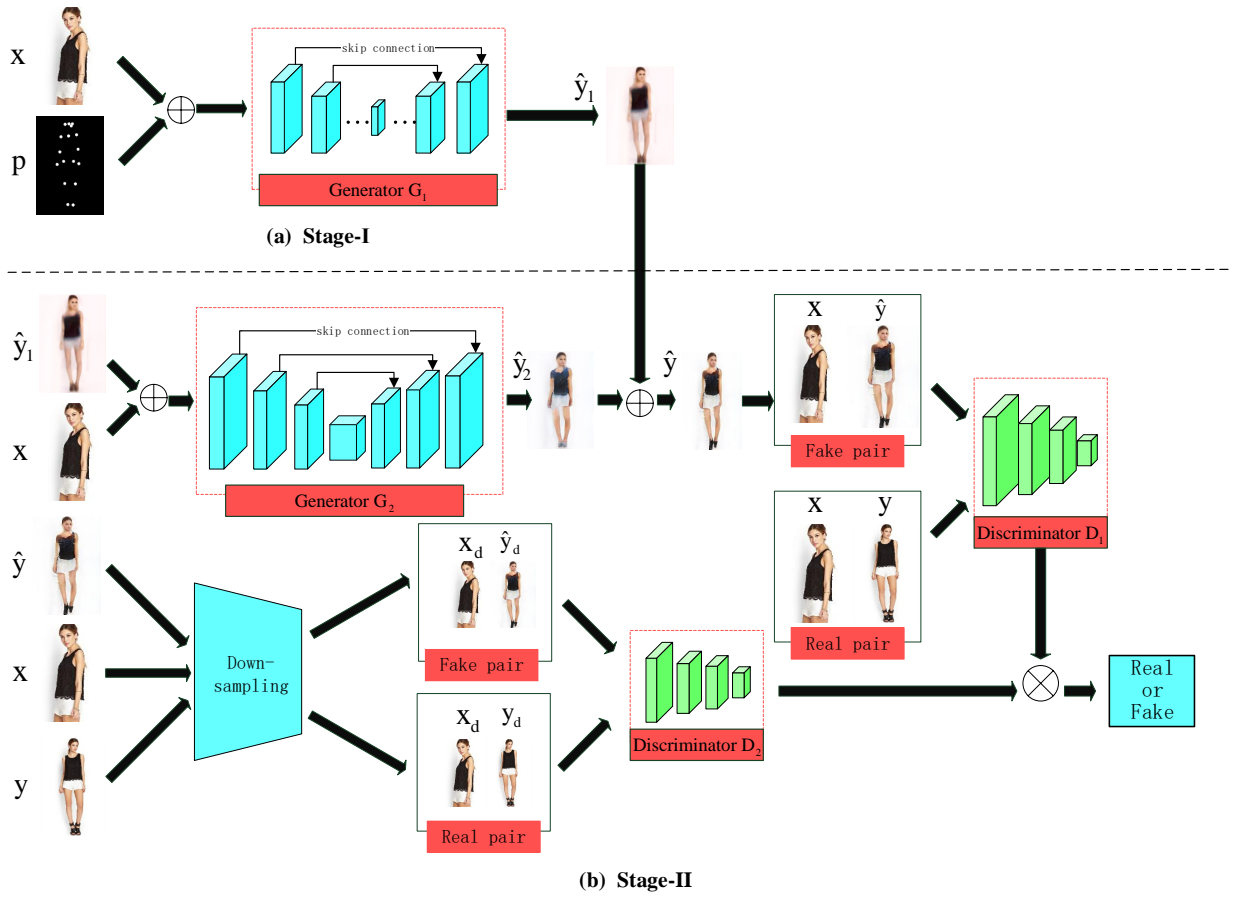


Fig. 2. The architecture of the proposed Multi-scale Conditional Generative Adversarial Networks (MsCGAN). It contains two stages. The Stage-I is show in (a), where global structure generator G_1 generate a coarse image (\hat{y}_1). The Stage-II is show in (b), where the local reinforcement generator G_2 conditioned on Stage-I results enhances the appearance details of the person and the texture information of the conditional person image, yielding a more realistic high-resolution image. The discriminators D_1 and D_2 discriminate the image pair which are original size and the downsampled image pair, respectively. Finally, weighted sum of the two discriminants results are taken as the discriminant result.

local reinforcement generator and multi-scale discriminators to obtain more details of the person and the texture information of the conditional person image. The proposed MsCGAN can synthesize images with high pose accuracy and realistic detail compared to existing techniques.

3 METHOD

TABLE 1 lists the key notations for the proposed MsCGAN which will be used in the following parts. The architecture of MsCGAN is shown in Fig. 2. In summary, the global-to-local generators consist of two generators which integrate coarse image and enhance refined images respectively. To obtain more details of the person and the texture information of the conditional person image, we apply the multi-scale discriminators consisting of two discriminators that discriminate images of different resolutions. Overall, MsCGAN contains two stages and they will be detailed respectively as follows:

3.1 Stage-I: Global Generation

At stage-I, we input the conditional person image (x) and the human pose estimation of target person image (p) to synthesize a global structure image (\hat{y}_1) containing the pose of the target person image (y).

TABLE 1
List of key notations.

Notation	Description
x	conditional person image
y	target person image
p	pose of target person image
\hat{y}_1	the result of stage-I
\hat{y}_2	the result of stage-II
\hat{y}	the final synthetic image
x_d	the image after downsampling x
y_d	the image after downsampling y
\hat{y}_d	the image after downsampling \hat{y}
\oplus	concatenation
\otimes	weighted sum

3.1.1 Human Pose Estimation

Here we use Part Affinity Fields (PAFs) method [14] to obtain highly accurate map of human pose estimation in real time. PAFs is flexible and robust since the method detects keypoints firstly and then classifies the keypoints as corresponding body parts. In our work, PAFs estimates the human pose in the conditional person image and generates the coordinates of eighteen 2D keypoints in real time. Then we encode the eighteen 2D keypoints into eighteen heatmaps to express the human pose more intuitively.

3.1.2 Generator G_1 : Full Person Image Generator

Generator G_1 adopts a variant of the U-Net network [11] and the residual blocks [15]. The input of G_1 is a concatenation of the conditional person image (x) and the map of human pose estimation generated by the target person image (p), while the output of G_1 is a coarse image (\hat{y}_1) with pose of the target person image. The poses of the x and the (\hat{y}_1) are quite different, but they are closely related to the appearance feature of the person. To change the pose of the person and preserve the detailed appearance of the person simultaneously, we employ skip connection between the symmetric layers of encoder and decoder in the variant of U-Net network. Since the generated image using L_2 distance is more blurred than that using L_1 distance in generator [16], we use L_1 distance as its basic loss function.

3.1.3 Compensation for the Impact of Background

The generators originally have no idea the background of generates image should be like, which would cause the results unrealistic. Furthermore, when the input image is unsharp, the person and the background are prone to jumble. In order to mitigate the impact of background, we adopt two strategies. First, we connect 18 heatmaps and fill the human body with 1 by geometric transformation to increase its area proportion in the image (shown in Fig. 3). Second, we introduce the background loss that uses the pose mask of the target person image (M_p) to separate the person when calculating L_1 loss. In the M_p , 1 indicates the person and 0 indicates the background.

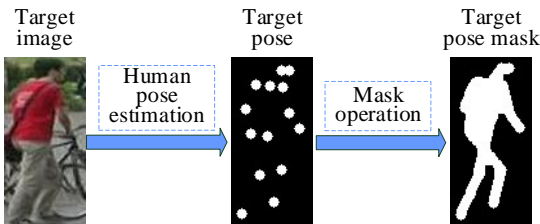


Fig. 3. Illustration of converting target person image to target pose mask.

3.1.4 Overall Loss Function for Stage-I

According to the above description, the loss of generator G_1 consists of L_1 loss and background loss. Thus, the overall loss function for Stage-I is formulated as:

$$\begin{aligned} \mathcal{L}_{Stage_1} &= \mathcal{L}_{L1_1} + \lambda_{bg_1} \mathcal{L}_{bg_1} \\ &= \|y - G_1(x, p)\|_1 + \lambda_{bg_1} \| (y - G_1(x, p)) \odot p_m \|_1, \end{aligned} \quad (1)$$

here $\|y - G_1(x, p)\|_1$ and $\|y - G_1(x, p) \odot P_m\|_1$ indicate L_1 loss and background loss, λ_{bg_1} is a hyperparameter that indicates the weight of background loss, and \odot denotes the pixels-wise multiplication.

Although \hat{y}_1 contains the global structure information of the target person image (y), it is blurry due to the inherent shortcomings of L_1 distance. Therefore, we need to enhance \hat{y}_1 in the second stage to make it could inherit more appearance features and texture information from the conditional person image.

3.2 Stage-II: Local Reinforcement

At stage-II, we correct the detailed feature of \hat{y}_1 and discriminate the synthetic image. We design a local reinforcement generator G_2 to generate an appearance difference map (\hat{y}_2) between x and \hat{y}_1 . Then, \hat{y}_1 and \hat{y}_2 are merged into the final synthetic image (\hat{y}). Multi-scale discriminators consist of two discriminators that discriminate different resolution versions of the synthetic image. We adopt a conditional DCGAN-like network as our base model and deem \hat{y}_1 as its condition.

3.2.1 Generator G_2 : Local Reinforcement Generator

Local reinforcement generator G_2 is a network inspired by conditional DCGAN and U-Net architectures. Specifically, the encoder of G_2 is a variant of the conditional DCGAN network [17] and is symmetric to the decoder of G_2 . The inputs of G_2 are the conditional person image (x) and the stage-I generation result (\hat{y}_1), while the output of G_2 is an appearance difference map (\hat{y}_2) between x and \hat{y}_1 . The fully connected layer destroys the spatial structure of the image while compressing it. The DCGAN network is a full-convolution architecture so that the details of the image can be preserved more completely.

3.2.2 Multi-scale Discriminators

In order to generate a high-resolution image, it is necessary to increase the receptive field of the discriminator. To increase the number and complexity of network may lead to overfitting and challenges for training. Addressing this, we adopt multi-scale discriminators which consist of two discriminators (D_1 and D_2) that discriminate different resolution versions of the synthetic image. D_1 is used the same network structure to D_2 , however, the only difference between D_1 and D_2 is different size of their input image. We downsample the conditional person image (x), the final synthetic image (\hat{y}) and the target person image (y) by a factor of 2 to create an image pyramid with 2 scales. The discriminators D_1 and D_2 are trained to distinguish real and synthesized images at the 2 different scales, respectively. Since the input of G_2 are the conditional person image (x) and the generation result (\hat{y}_1) of stage-I, the pose in the image generated by G_2 may be similar to the pose in the x . In order to avoid this scenario, we 1) input x replacing a random noise into the discriminator D_1 in pairs with y and \hat{y}_1 respectively. 2) Operate the images which are downsampled by a factor of 2 in the same way as the inputs of D_2 .

3.3 Overall Loss Function for Stage-II

At stage-II, we use conditional GAN as our basic loss function, and add L_1 loss, background loss which introduced in stage-I as extra supervisory signals.

The loss function of the conditional GAN is formulated as:

$$\begin{aligned} \mathcal{L}_{cGAN}(G, D) &= \\ &= \mathbb{E}_{x,y}[\log D(x, y)] + \mathbb{E}_{x,z}[\log(1 - D(x, G(x, z)))], \end{aligned} \quad (2)$$

where z refers to $G_1(x, p)$. G tries to minimize this objective against an adversarial D which tries to maximize it.

Therefore, the loss function of the conditional GAN can be optimized as following:

$$\min_{G_2} \max_{D_1, D_2} (\lambda_{D_1} \mathcal{L}_{cGAN}(G_2, D_1) + \lambda_{D_2} \mathcal{L}_{cGAN}(G_2, D_2)), \quad (3)$$

where λ_{D_1} and λ_{D_2} control the importance of the two terms, respectively.

Thus, our full loss combining conditional GAN loss, L_1 loss and background loss for Stage-II is formulated as:

$$\begin{aligned} \mathcal{L}_{Stage_2} = & \min_{G_2} (\max_{D_1, D_2} (\lambda_{D_1} \mathcal{L}_{cGAN}(G_2, D_1) + \\ & \lambda_{D_2} \mathcal{L}_{cGAN}(G_2, D_2)) + \lambda_{L1,2} \|y - G_2(x, G_1(x, p))\|_1 \\ & + \lambda_{bg,2} \|y - G_2(x, G_1(x, p)) \odot p_m\|_1), \end{aligned} \quad (4)$$

where $\lambda_{L1,2}$ and $\lambda_{bg,2}$ are the weights of L_1 loss and background loss.

3.4 Network Architectures

Here we give the detailed description of the proposed MsCGAN. The network architectures consist of four main components: generators G_1 , G_2 , discriminators D_1 and D_2 .

3.4.1 Network Architectures of Generators

The encoder of G_1 consists of $M-1$ residual blocks and one fully connected layer. The last residual block of encoder is composed of two convolutional layers with stride=1. Each of the remaining residual blocks consists of two convolutional layers with stride=1 and a convolutional layer with stride=2.

The encoder of G_2 is a full convolutional network consisting of $M-2$ convolutional blocks. The last convolutional block of encoder is composed of two convolutional layers with stride=1. Each of the remaining convolutional blocks consists of two convolutional layers with stride=1 and a convolutional layer with stride=2. In G_1 and G_2 , the filters of all convolutional layers are $3*3$ and $4*4$, and the number of filters increases linearly in the encoder.

The decoders of G_1 and G_2 are symmetric with the corresponding encoder, respectively. There are skip connections between encoders and decoders, but no batchnorm or dropout. Rectified linear units (ReLU) [18] are used for all layers except the full connection layer and the output convolution layer.

3.4.2 Network Architectures of Discriminators

The architectures of our discriminators are inspired by the previous DCGAN, and D_1 has the same network structure as D_2 . The network structures of discriminator D_1 and D_2 consist of $M-1$ convolutional layers, each of which consists of a convolution with $4 * 4$ filters, stride=2 and padding=1. Leaky rectified linear units (LeakyReLU) [19] are applied to all convolution layer while we use batchnorm [20] for all convolutional layers except the first convolutional layer. The final output is a one-dimensional value which indicates that the discriminators evaluate the authenticity of the input images.

Our networks have some differences from the input layer of DCGAN [17] in term of the sizes of the input images. The input of the discriminator D_1 are color image of $128 * 64$ for Market-1501 dataset and $256 * 256$ for DeepFashion dataset respectively, while D_2 is a color image of

$64*32$ for Market-1501 dataset and $128*128$ for DeepFashion dataset respectively.

The size of M is determined by the size of the input image. When the size of input image is $128*64$, $M=5$. When the size of input image is $256 * 256$, $M=6$. The detailed network architectures of MsCGAN are shown in the appendix.

4 EXPERIMENTS

This section demonstrates the effectiveness of the proposed MsCGAN. We firstly introduce datasets and implementation details. Then, we show the qualitative and quantitative evaluations of the proposed MsCGAN.

4.1 Datasets

We conduct evaluations on two public datasets: a low-resolution person re-identification dataset (Market-1501 dataset [12]) and a high-resolution fashion photo dataset (DeepFashion dataset [13]) due to person images on these datasets have various poses.

Market-1501 is a person re-identification dataset and contains 32668 images of 1501 persons with resolution of $128 * 64$, which are captured from six different surveillance cameras. Images in Market-1501 have a high diversity in background, character pose, shooting angle and lighting. We separate the training set and the test set into 12936 and 19732 images. In order to train the model using paired data, we convert the train set into 439420 pairs of data for the same person but different poses. The test set is processed in same way and randomly selected 12800 pairs for testing.

DeepFashion (In-shop Clothes Retrieval Benchmark) dataset consists of 52,712 clothes images with resolution of $256 * 256$. Each image is matched with all others to construct 200,000 pairs of identical clothes, which two different poses and/or scales of the persons wearing these clothes [13]. We separated the training set into 146680 pairs of images for the same person but different poses. Test set is processed in the same way and randomly selected 12800 pairs for testing.

4.2 Implementation Details

Our MsCGAN is implemented with Tensorflow [21] and we apply the Adam optimizer [22] with adapted hyper-parameters. After several experiments, we find that the default parameters (learning rate is 0.001, momentum parameters $\beta_1 = 0.9$ and $\beta_2 = 0.99$) result in training oscillation and instability. Therefore, we set learning rate to 0.0001, momentum parameters $\beta_1 = 0.5$ and $\beta_2 = 0.9$ to obtain stable and realistic images. As suggested in [6], we improve the gradient by training to maximize $\log D(x, G(x, z))$ rather than minimize $\log(1 - D(x, G(x, z)))$ in the implementation.

4.3 Baselines

To demonstrate the proposed MsCGAN can achieve superior results, we compare our method with three state-of-the-art works: [7], [9] and [10].

Moreover, to demonstrate the proposed network structure proposed in Section 3 is optimal, we evaluate qualitative and quantitative results of three settings: One discriminator, Two discriminators (MsCGAN) and Three discriminators. All of them have the same global-to-local generators

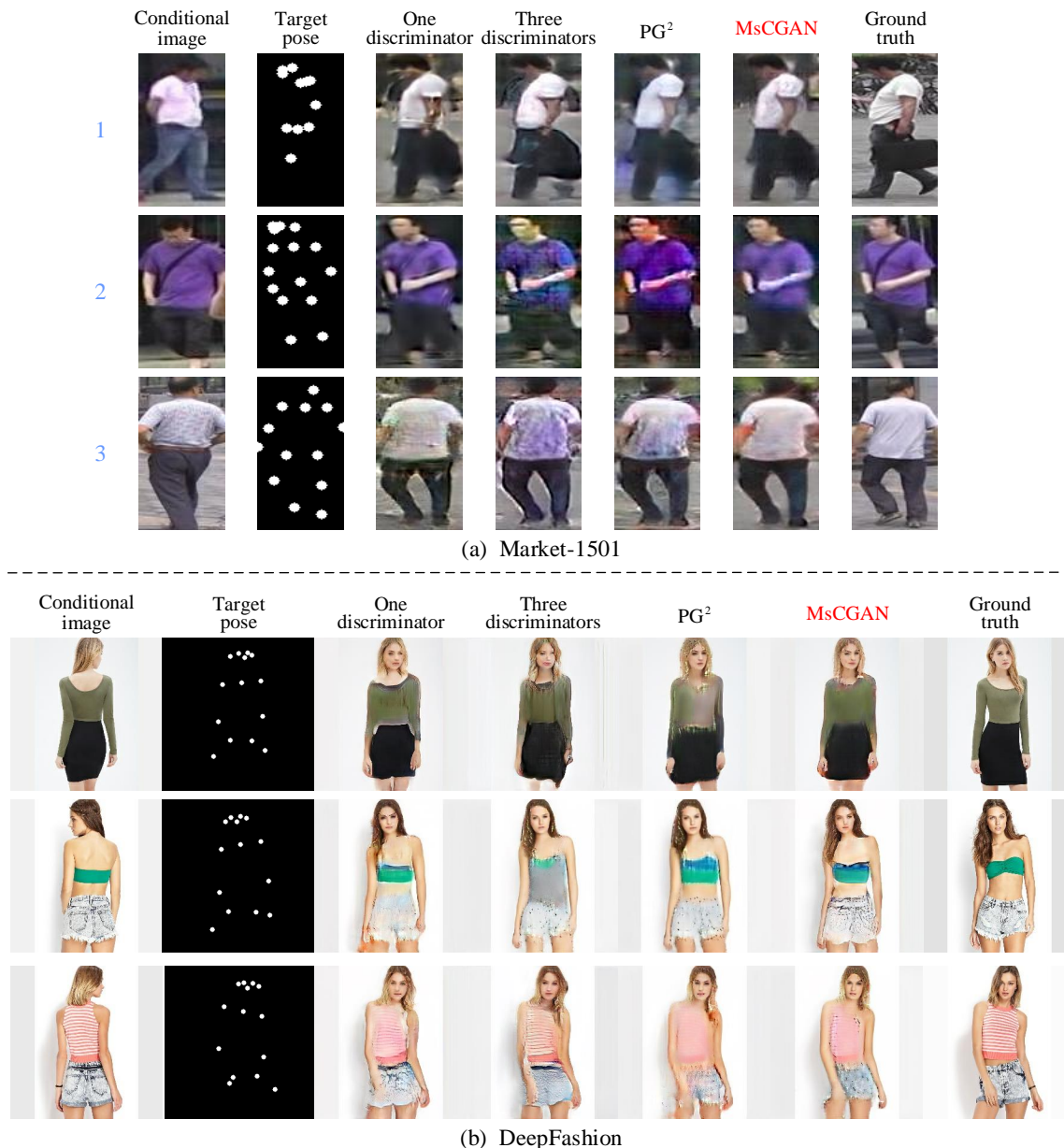


Fig. 4. Example of results on Market-1501 dataset and DeepFashion dataset.

while the number of discriminators are different, the setting details are as follows:

One discriminator has only one discriminator and its inputs are real pair and fake pair. The former consists of the final synthetic image (\hat{y}) and conditional person image (x), while the latter consists of target person image (y) and conditional person image (x).

Two discriminators (MsCGAN) have two discriminators and one of them is exactly the same as the one in One discriminator. We downsample the conditional person image (x), the final synthetic image (\hat{y}) and the target person image (y) by a factor of 2. The inputs of the other are real pair and fake pair which consist of downsampled images.

Three discriminators have three discriminators and two of them are exactly the same as the discriminators in Two discriminators. We downsample the conditional person im-

age (x), the final synthetic image (\hat{y}) and the target person image (y) by a factor of 4. The inputs of the remaining one are real pair and fake pair which consists of downsampled images.

Note that we use the same generators, the same datasets and the same hyper-parameters to train and test all baselines mentioned above.

4.4 Results and Discussions

4.4.1 Qualitative Results

We apply global-to-local generators and multi-scale discriminators consisting of two discriminators. To illustrate the difference of using two discriminators and using one, or three discriminators, we perform different number of discriminators for qualitative comparisons. Moreover, we

TABLE 2
Quantitative results on two public datasets, higher scores are better.

Model	DeepFashion		Market-1501			
	SSIM	IS	SSIM	IS	mask-SSIM	mask-IS
One discriminator	0.737	3.212	0.248	3.167	0.791	3.246
MsCGAN	0.725	3.335	0.219	3.588	0.764	3.741
Three discriminators	0.691	3.284	0.216	3.459	0.778	3.558
Ma et al. NIPS2017 [7]	0.762	3.090	0.253	3.460	0.792	3.435
Ma et al. CVPR2018 [10]	0.614	3.228	0.099	3.483	0.614	3.491
Pumarola et al. CVPR2018 [9]	0.747	2.97	—	—	—	—

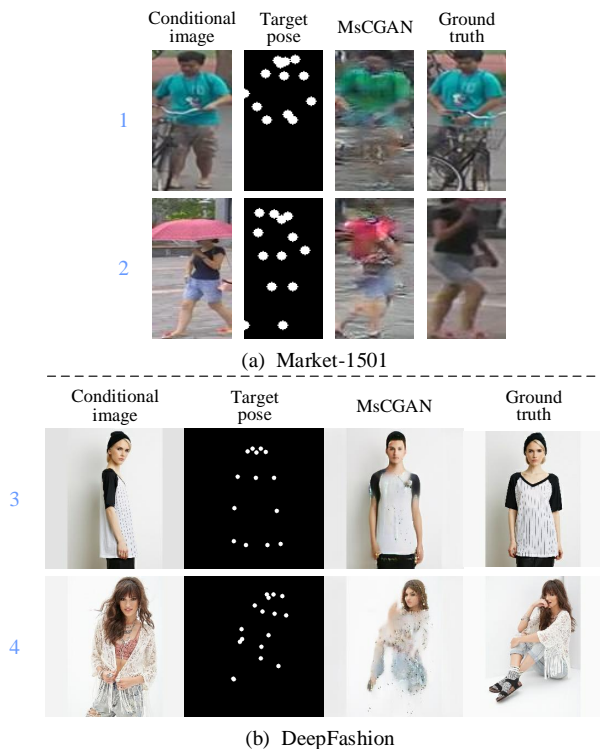


Fig. 5. A few typical failure cases on Market-1501 dataset and DeepFashion dataset.

compare our results with PG^2 [7]. The results for different models are shown in Fig. 4.

From the Fig. 4, it is clear that MsCGAN can generate more photo-realistic results than other methods. For Market-1501 samples, since both conditional person image and target person image are low resolution, the final synthetic image is not very clear but has the pose of target person image at first glance. And even so, from 1-th and 2-th rows, we can still observe that MsCGAN is able to generate approximate outline of a black handbag.

For DeepFashion samples, it is obvious that the generated image by MsCGAN is closer to the ground truth than other methods. The major reason is that our MsCGAN plays more attention on appearance and texture information of the conditional person image.

4.4.2 Quantitative Results

We adopt the same evaluation protocol from previous person image generation works [7] [23] [10] [24]. We use Structural Similarity Index Measure (SSIM) [25] and Inception Score (IS) [26] and their corresponding masked versions

mask-SSIM and mask-IS [7]. SSIM calculates image similarity by combining luminance comparison, contrast comparison and structure comparison between the synthetic image and the ground truth. The range of SSIM is $[0, 1]$, and high SSIM value indicates high structural similarity. Inception Score (IS) is a common metric for evaluation that correlates with human judgment closely. IS captures the uniqueness of a single sample and the differences between multiple samples to evaluate the synthetic image. Its objective and controllable to evaluate the IS on a large enough number of samples [26]. Since the generators don't know what kind of background to generated image would be like, we calculate mask-SSIM and mask-IS by masking-out the image background to alleviate the impact of the background. The evaluation masks have been established in accordance with the procedure presented in [7]. Quantitative results are shown in TABLE 2.

From the TABLE 2, it is clear that MsCGAN achieves the highest score in IS and mask-IS criteria. Moreover, we can see that the generated images of the three discriminators are not as good as the images generated by the two discriminators. There are two main reasons for this phenomenon: 1) continuous downsampling will destroy the spatial structure of the image. 2) For images with low resolution, continuous downsampling will extract invalid feature information.

4.4.3 Failure Cases

Although MsCGAN can synthesize more photo-realistic results than other methods, it still has failure cases. We select a few typical failure cases which are shown in Fig. 5. From the result in the row 1, we can see that objects in the conditional person image have a great influence on human pose estimation so the proposed MsCGAN synthesizes poor-quality result. From the result in the row 2, the occlusion of the person in the conditional person image causes the appearance of the synthetic image to be disorganized.

In the row 3, we can find that MsCGAN causes an error of gender which transforms female into male. In the row 4, the body in the target person image does not appear in the conditional person image, resulting in an incomplete body of the generated image.

Therefore, we think there are two main reasons why image generation fails. The first one is that the conditional person image is too blurred and there are else objects in it, which affects the detection of keypoints on the human body. The second one is that the conditional person image is occluded, which affects the appearance features and texture information of the synthetic image.

5 CONCLUSION

In this paper, we propose a novel multi-scale conditional generative adversarial networks (MsCGAN) for generating high-quality and photo-realistic person image with arbitrary poses. The proposed MsCGAN can simultaneously model target pose as well as the the appearance of the conditional person image in a unified and principled way. In experiments, the qualitative and quantitative results clearly demonstrate the effectiveness of the proposed model. In the future, we will evaluate our model on more practical datasets and investigate more applications.

REFERENCES

- [1] Z. Zheng, L. Zheng, and Y. Yang, "Unlabeled samples generated by gan improve the person re-identification baseline in vitro," *arXiv preprint arXiv:1701.07717*, vol. 3, 2017.
- [2] C. Si, W. Wang, L. Wang, and T. Tan, "Multistage adversarial losses for pose-based human image synthesis," in *Proceedings of the IEEE Conference on Computer Vision and Pattern Recognition*, 2018, pp. 118–126.
- [3] J. Walker, K. Marino, A. Gupta, and M. Hebert, "The pose knows: Video forecasting by generating pose futures," in *Computer Vision (ICCV), 2017 IEEE International Conference on*. IEEE, 2017, pp. 3352–3361.
- [4] D. P. Kingma and M. Welling, "Auto-encoding variational bayes," *arXiv preprint arXiv:1312.6114*, 2013.
- [5] A. v. d. Oord, N. Kalchbrenner, and K. Kavukcuoglu, "Pixel recurrent neural networks," *arXiv preprint arXiv:1601.06759*, 2016.
- [6] I. Goodfellow, J. Pouget-Abadie, M. Mirza, B. Xu, D. Warde-Farley, S. Ozair, A. Courville, and Y. Bengio, "Generative adversarial nets," in *Advances in neural information processing systems*, 2014, pp. 2672–2680.
- [7] L. Ma, X. Jia, Q. Sun, B. Schiele, T. Tuytelaars, and L. Van Gool, "Pose guided person image generation," in *Advances in Neural Information Processing Systems*, 2017, pp. 406–416.
- [8] A. Siarohin, E. Sangineto, S. Lathuilière, and N. Sebe, "Deformable gans for pose-based human image generation," in *CVPR 2018-Computer Vision and Pattern Recognition*, 2018.
- [9] A. Pumarola, A. Agudo, A. Sanfeliu, and F. Moreno-Noguer, "Unsupervised person image synthesis in arbitrary poses," in *Proceedings of the IEEE Conference on Computer Vision and Pattern Recognition*, 2018, pp. 8620–8628.
- [10] L. Ma, Q. Sun, S. Georgoulis, L. Van Gool, B. Schiele, and M. Fritz, "Disentangled person image generation," in *Proceedings of the IEEE Conference on Computer Vision and Pattern Recognition*, 2018, pp. 99–108.
- [11] O. Ronneberger, P. Fischer, and T. Brox, "U-net: Convolutional networks for biomedical image segmentation," in *International Conference on Medical image computing and computer-assisted intervention*. Springer, 2015, pp. 234–241.
- [12] L. Zheng, L. Shen, L. Tian, S. Wang, J. Wang, and Q. Tian, "Scalable person re-identification: A benchmark," in *Proceedings of the IEEE International Conference on Computer Vision*, 2015, pp. 1116–1124.
- [13] Z. Liu, P. Luo, S. Qiu, X. Wang, and X. Tang, "Deepfashion: Powering robust clothes recognition and retrieval with rich annotations," in *Proceedings of the IEEE conference on computer vision and pattern recognition*, 2016, pp. 1096–1104.
- [14] Z. Cao, T. Simon, S.-E. Wei, and Y. Sheikh, "Realtime multi-person 2d pose estimation using part affinity fields," *arXiv preprint arXiv:1611.08050*, 2016.
- [15] K. He, X. Zhang, S. Ren, and J. Sun, "Deep residual learning for image recognition," in *Proceedings of the IEEE conference on computer vision and pattern recognition*, 2016, pp. 770–778.
- [16] P. Isola, J.-Y. Zhu, T. Zhou, and A. A. Efros, "Image-to-image translation with conditional adversarial networks," *arXiv preprint*, 2017.
- [17] A. Radford, L. Metz, and S. Chintala, "Unsupervised representation learning with deep convolutional generative adversarial networks," *arXiv preprint arXiv:1511.06434*, 2015.
- [18] G. E. Dahl, T. N. Sainath, and G. E. Hinton, "Improving deep neural networks for lvcsr using rectified linear units and dropout," in *Acoustics, Speech and Signal Processing (ICASSP), 2013 IEEE International Conference on*. IEEE, 2013, pp. 8609–8613.
- [19] T. Zhou *et al.*, "A study of generative adversarial networks and possible extensions of gans," Ph.D. dissertation, 2017.
- [20] S. Ioffe and C. Szegedy, "Batch normalization: Accelerating deep network training by reducing internal covariate shift," *arXiv preprint arXiv:1502.03167*, 2015.
- [21] M. Abadi and A. A. B. P. TensorFlow, "Large-scale machine learning on heterogeneous distributed systems," in *Proceedings of the 12th USENIX Symposium on Operating Systems Design and Implementation (OSDI16)(Savannah, GA, USA, 2016*, pp. 265–283.
- [22] D. P. Kingma and J. Ba, "Adam: A method for stochastic optimization," *arXiv preprint arXiv:1412.6980*, 2014.
- [23] J. Johnson, A. Alahi, and L. Fei-Fei, "Perceptual losses for real-time style transfer and super-resolution," in *European Conference on Computer Vision*. Springer, 2016, pp. 694–711.
- [24] W. Shi, J. Caballero, F. Huszár, J. Totz, A. P. Aitken, R. Bishop, D. Rueckert, and Z. Wang, "Real-time single image and video super-resolution using an efficient sub-pixel convolutional neural network," in *Proceedings of the IEEE Conference on Computer Vision and Pattern Recognition*, 2016, pp. 1874–1883.
- [25] Z. Wang, A. C. Bovik, H. R. Sheikh, and E. P. Simoncelli, "Image quality assessment: from error visibility to structural similarity," *IEEE transactions on image processing*, vol. 13, no. 4, pp. 600–612, 2004.
- [26] T. Salimans, I. Goodfellow, W. Zaremba, V. Cheung, A. Radford, and X. Chen, "Improved techniques for training gans," in *Advances in Neural Information Processing Systems*, 2016, pp. 2234–2242.

APPENDIX

We list the detailed network architectures of MsCGAN in the following tables. The key notations for the abbreviated words which represent the network structures are shown in TABLE 3. Since network layers of MsCGAN depend on the size of the input images, MsCGAN is a novel model with variational network layers.

TABLE 3
List of key notations for the abbreviated words.

Notation	Description
Ker	Kernel
Str	Stride
Pad	Padding
Act fn	Activation function
Out_M	Out channels for Market-1501 dataset
Out_D	Out channels for DeepFashion dataset
CONV	Convolutional layer
DECONV	Deconvolutional layer
CONV BLOCK	Convolutional block
Res BLOCK	Residual block
FC	Fully connected layer
BN	Batchnorm

A The Network Architectures of Generator G_1

The network architectures of G_1 are shown in TABLE 4 and TABLE 5. *CONV2*, *Res BLOCK5*, *DECONV1* and *Res BLOCK5* are only for DeepFashion dataset. The rest of the network structures are applicable to both Market-1501 dataset and DeepFashion dataset. In the decoder, the last layer of the first three residual blocks is a deconvolutional layer which is used to enlarge the generated images.

TABLE 4
The encoder of G_1 .

Layer	Ker	Str	Pad	Act fn	Out_M	Out_D
CONV1	3*3	1	1	ReLU	128	128
Res BLOCK1	3*3	1	1	ReLU	128	128
	3*3	1	1	ReLU	128	128
	3*3	2	1	ReLU	256	256
Res BLOCK2	3*3	1	1	ReLU	256	256
	3*3	1	1	ReLU	256	256
	3*3	2	1	ReLU	512	512
Res BLOCK3	3*3	1	1	ReLU	512	512
	3*3	1	1	ReLU	512	512
	3*3	2	1	ReLU	1024	1024
Res BLOCK4	3*3	1	1	ReLU	1024	1024
	3*3	1	1	ReLU	1024	1024
CONV2	3*3	2	1	ReLU	—	2048
Res BLOCK5	3*3	1	1	ReLU	—	2048
	3*3	1	1	ReLU	—	2048
FC	—	—	—	—	64 dims	64 dims

B The Network Architectures of Generator G_2

The network architectures of G_2 are shown in TABLE 6 and TABLE 7. *CONV2*, *CONV BLOCK4*, *DECONV1* and *CONV BLOCK4* are only for DeepFashion dataset. Similarly to G_1 , the rest of the network structures are applicable to both two datasets and the last layer of the first two convolutional blocks is a deconvolutional layer.

TABLE 5
The decoder of G_1 .

Layer	Ker	Str	Pad	Act fn	Out_M	Out_D
FC	—	—	—	—	4096 dims	4096 dims
Res BLOCK1	3*3	1	1	ReLU	1024	2048
	3*3	1	1	ReLU	1024	2048
	3*3	2	1	ReLU	512	1024
Res BLOCK2	3*3	1	1	ReLU	512	1024
	3*3	1	1	ReLU	512	1024
	3*3	2	1	ReLU	256	512
Res BLOCK3	3*3	1	1	ReLU	256	512
	3*3	1	1	ReLU	256	512
	3*3	2	1	ReLU	128	256
Res BLOCK4	3*3	1	1	ReLU	128	256
	3*3	1	1	ReLU	128	256
DECONV1	3*3	2	1	ReLU	—	128
Res BLOCK5	3*3	1	1	ReLU	—	128
	3*3	1	1	ReLU	—	128
CONV2	3*3	1	1	ReLU	3	3

TABLE 6
The encoder of G_2 .

Layer	Ker	Str	Pad	Act fn	Out_M	Out_D
CONV1	3*3	1	1	ReLU	128	128
CONV BLOCK1	3*3	1	1	ReLU	128	128
	3*3	1	1	ReLU	128	128
	4*4	2	1	ReLU	256	256
CONV BLOCK2	3*3	1	1	ReLU	256	256
	3*3	1	1	ReLU	256	256
	4*4	2	1	ReLU	512	512
CONV BLOCK3	3*3	1	1	ReLU	512	512
	3*3	1	1	ReLU	512	512
CONV2	4*4	2	1	ReLU	—	1024
CONV BLOCK4	3*3	1	1	ReLU	—	1024
	3*3	1	1	ReLU	—	1024

TABLE 7
The decoder of G_2 .

Layer	Ker	Str	Pad	Act fn	Out_M	Out_D
CONV BLOCK1	3*3	1	1	ReLU	512	1024
	3*3	1	1	ReLU	512	1024
	4*4	2	1	ReLU	256	512
CONV BLOCK2	3*3	1	1	ReLU	256	512
	3*3	1	1	ReLU	256	512
	4*4	2	1	ReLU	128	256
CONV BLOCK3	3*3	1	1	ReLU	128	256
	3*3	1	1	ReLU	128	256
DECONV1	4*4	2	1	ReLU	—	128
CONV BLOCK4	3*3	1	1	ReLU	—	128
	3*3	1	1	ReLU	—	128
CONV1	3*3	1	1	ReLU	3	3

C The Network Architectures of Discriminators

The network architectures of Discriminators are shown in TABLE 8 and *CONV5* is just for DeepFashion dataset. The first four convolutional layers are applicable to both Market-1501 dataset and DeepFashion dataset.

TABLE 8
The network architectures of discriminators

Layer	Ker	Str	Pad	BN	Act fn	Output channels
CONV1	4*4	2	1	No	LeakyReLU	128
CONV2	4*4	2	1	Yes	LeakyReLU	256
CONV3	4*4	2	1	Yes	LeakyReLU	512
CONV4	4*4	2	1	Yes	LeakyReLU	1024
CONV5	4*4	2	1	Yes	LeakyReLU	2048